We A1 07

Improved Deep Target Reservoir Imaging with Broadband WATS Data in the East China Sea

H. Chen (CNOOC), S. Hu (CNOOC), Y. Wei (CNOOC), P. Deng* (CGG), Y. Xiao (CGG), W. Kuang (CGG), S. Cao (CGG), S. Poonamalli (CGG), R. To (CGG), J. Zhou (CGG), J. Sun (CGG), G. Yao (CNOOC), Y. Jiang (CNOOC)

Summary

A broadband Wide-Azimuth Towed-Streamer (WATS) survey was acquired in a shallow water region of offshore China for resolving strike direction narrow-azimuth acquisition shortcomings. This WATS acquisition is much sparser than WATS surveys in deep water environments due to the one-side WATS configuration. The combination of sparse acquisition, shallow water, and deep targets, require optimal utilization of the side-gun data as the key to final imaging improvements. A comprehensive flow for resolving the challenges of de-ghosting and de-multiple for sparse and shallow wide-azimuth data is presented in the paper. Side gun data clearly enhances the final target reservoir imaging and better ties the well by including dip direction information. Contribution analysis of side guns in this survey shows that better azimuth distribution shall play a more significant role than far offsets in the final imaging, which provides valuable guidance for future acquisition designs in similar geographical and geological conditions.

Introduction

Several wells were drilled into the target reservoir of a production field, located in a shallow water (70 - 110 m) region of the East China Sea. Most of the wells were successful except one. Careful analysis of the legacy seismic image shows that all of the wells should have been drilled into the same structure at depths between 3.1 - 3.6 km, therefore, it is concluded that the legacy data is not adequate for resolving reservoir compartments and new broadband data is needed. Legacy acquisition follows the dip direction, but unfortunately due to operational limitations, the new acquisition had to follow the strike direction as shown in Fig. 1(a). To overcome this shortcoming, two side boats were added as additional source boats to form a WATS acquisition geometry. The side guns provide the needed dip-direction reflection information.

As shown in Fig. 1(b), the WATS acquisition consists of 3 vessels, and 4 guns shooting in sequence. The acquisition was carried out in two passes. The streamer boat has 2 guns and 10 cables with 100 m cable separation, and 6 km cable length. The streamer profile is slanted for optimal notch diversity and better broadband data. The cable depth varies from 7 m in the near offset to 40 m in the far offset. The side boats each have 1 gun and are positioned laterally at 1 km and 2 km away from the streamer boat center-line for the 1st pass, and at 3 km and 4 km away for the 2nd pass. The streamer boat center-line shifts 12.5 m along the Crossline direction during the 2nd pass for better subsurface coverage. The inner side-boat is located 2km behind the 1st channel in the inline direction, rather than the center of the cable, to avoid possible entanglement from cable feathering, while the outer side-boat is located 3km behind the 1st channel. Fig. 1(c) shows the azimuth distribution of this acquisition geometry.

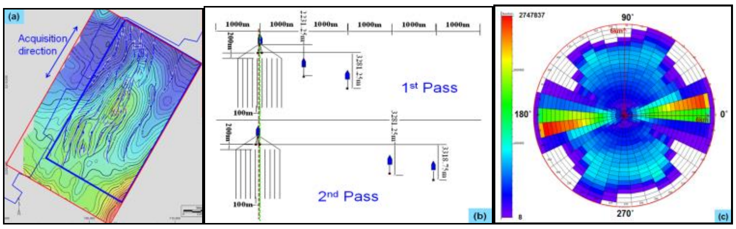

Figure 1: *(a) Survey Map; (b) Acquisition Geometry; (c) Rose Diagram*

Compared to WATS surveys in deep water environments such as the Gulf of Mexico (Michell at al. 2006), this acquisition is sparser due to the following two factors: the side boats are positioned only on one side of the streamer boat, and the distance between the side-boat and the steamer central line is quite large. With such sparse broadband wide-azimuth acquisition in a shallow water environment, the key issue is how to better process the data to obtain the full benefits of the additional source boats in terms of a better illumination and more effective multiple suppression. There are many challenges that must be overcome. Among them are de-ghosting and de-multiple, etc. We discuss these challenges in the next sections and demonstrate the full benefits of this broadband WATS acquisition.

De-ghosting

The 3D effect and severe aliasing expected in the Crossline direction must be addressed in order to fully utilize the side gun data. While 3D de-ghosting for side-gun data is not a new topic, especially in deep water regions (Wu et al. 2014, and Wang et al. 2014), shallow water depths pose additional issues and challenges for side-gun data de-ghosting. Refraction energy arrives early with abnormally strong amplitudes and mixes with the shallow primary reflections, leading to substantially inaccurate p estimations for the primary energy. Therefore, accurate 3D linear noise attenuation (LNA) is essential for better de-ghosting results. Fig. 2(a) is a shot gather just after 2.5Hz low-cut filtering and shows strong refraction linear noise masking the shallow. A progressive sparse Tau-p transform starting from low frequencies gives a feasible solution to the severe aliasing issues. Due to the strong 3D effect, 2D de-ghosting introduces ringing and leaves a lot of residual ghost energy in the data. Fig. 2(b) shows the same shot gather after 3D LNA, while Fig. 2(c) and (d) show a comparison between 2D and 3D de-ghosting results. The 3D de-ghosting effectively removes the ghost energy and reveals underlying multiples, seen as relatively flat trough energy on the autocorrelation. In addition to the early-arrival of strong refraction energy, the shallow water multiple notch frequency and receiver-side ghost notch frequency may overlap in certain areas on far channels with deep cable depths. For this reason, different domain de-ghosting QC may be necessary for better multiple and ghost energy discrimination.

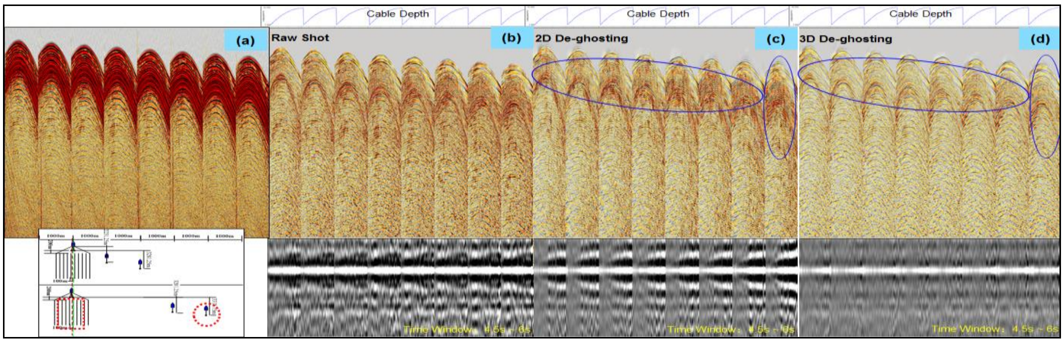

Figure 2: *Side-gun shot gather: (a) after 2.5Hz low cut; (b) after 3D LNA; (c) after 2D de-ghosting; (d) after 3D de-ghosting.*

De-multiple

WAZ data is known to better stack out multiples relative to narrow-azimuth data (VerWest and Lin 2007). This suppression phenomena comes from the mid to far offset trace contribution, which presents the multiples with more of a linear moveout that is much easier to stack out than a parabolic moveout. A natural question then, is whether the multiple suppression is still obvious when the acquisition is sparse and the water bottom is shallow such that multiple and primary move-out separation is obscure. Fig.3 shows a comparison of different stacks from the WATS data after de-ghosting: (a) presents a NAZ stack containing only main gun data with clear water-layer related 1st bounce multiple observed on the autocorrelation; (b) shows a stack with both the main gun data and the 1st pass side gun data with a clear suppression effect of the 1st bounce multiple energy; (c) shows a stack with all the main and side gun data where the multiple energy is further attenuated.

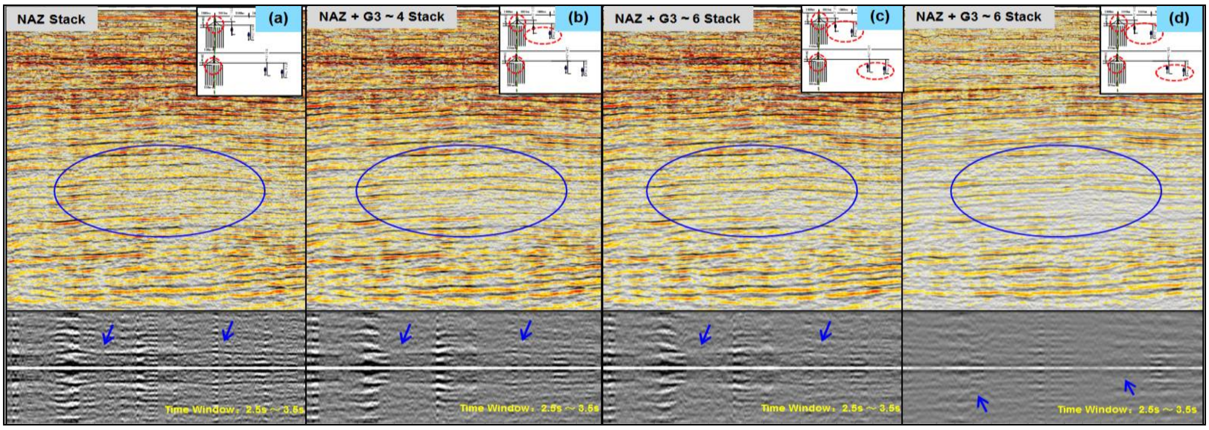

Figure 3: *Stack after de-ghosting: (a) NAZ with only main gun data, (b) NAZ+1st Pass side gun data, (c) NAZ+2 Passes side gun data; (d) NAZ+2 Passes side gun data: Stack after de-multiple.*

This comparison clearly confirms the multiple suppression capability of a sparse WATS data in a shallow water case. Nevertheless, an effective de-multiple processing flow is still crucial for the residual multiples and the final gather quality. The de-multiple flow applied for the survey is 3D Model-based Water-layer De-multiple (MWD), for cases when the water bottom reflection is poorly recorded. 3D SRME is used to target longer period multiples. Fig.3(c) and (d) show the full stack before and after the 3D de-multiple flow. The residual multiples are further eliminated.

Discussion on Contribution Analysis

To analyze the side gun contributions, comparison was done after improving migration results by 4D regularization (Wang and Wang, 2014), which avoids migration artefacts due to insufficient offset regularization. A gentle orthorhombic velocity model was built afterwards for better fault imaging and more accurate fault positioning despite weak azimuthal anisotropy.

Fig.4 shows an extracted RMS amplitude map from the target horizon around 3.5km deep from different stack volumes. Fig. 4(a) and (d) are from the NAZ case using only data sourced by the guns on the streamer vessel; while (b), (e) and (c), (f) further incorporate the 1st pass of side-gun data and then both passes of side-gun data respectively. The 1st pass side gun contributes dramatically to the final reservoir structural imaging and S/N improvement, while the 2nd pass contribution becomes less remarkable. Adaptive subtraction between these final PSDM images was used to evaluate the relative differences. A quantitative S/N calculation based on trace coherency was also derived. These different analyses all show the significant uplifts from the 1st pass of side-gun data and less significant contribution from the 2nd pass. Side gun data in general gives more spatial constraints for better velocity updates, but due to the very weak azimuthal anisotropy in the region, the contribution for velocity updates from 2nd pass is also limited. This analysis provides valuable guidance for future survey design in similar geology with limited budget where putting the 2nd pass side gun nearer to the streamer center line for better azimuth distribution, rather than further away for better longer offset distribution, could be considered.

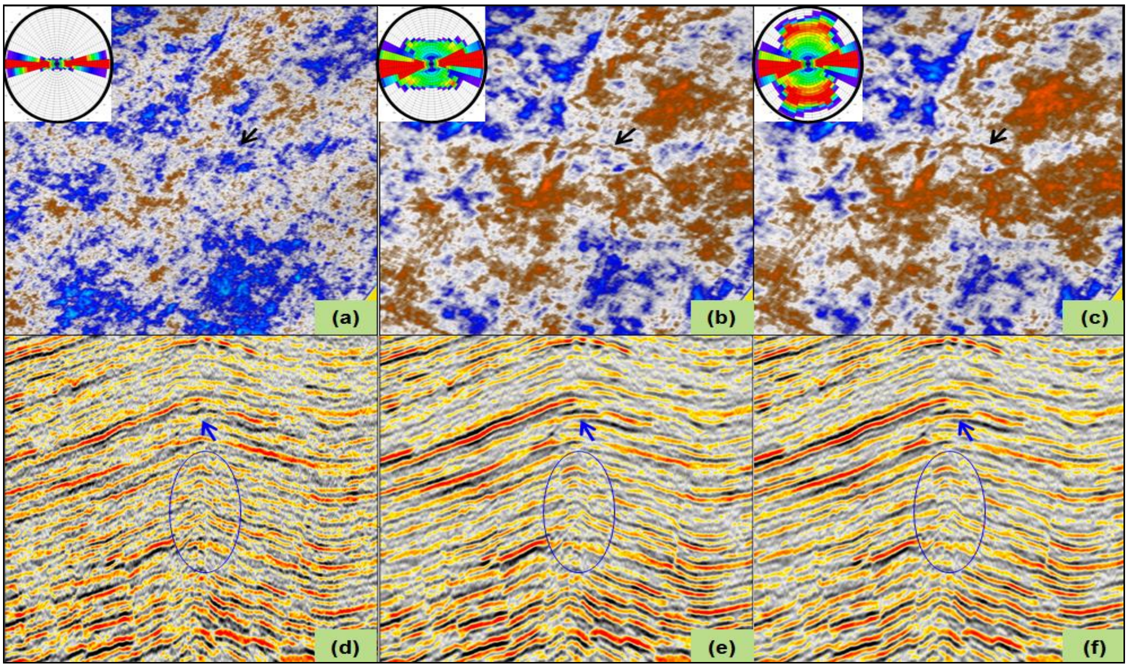

Figure 4: *Contribution of side guns on PSDM stacks (d, e, f) and related RMS amplitude maps (a, b, c) at a target reservoir horizon: (a, d) NAZ only, (b, e) NAZ+1st Pass side gun data and (c, f) NAZ+2 Passes side gun data.*

Final Results

The WATS final PSDM image has improved the S/N, broadened the bandwidth and improved the fault imaging significantly relative to the legacy image - see Fig. 5(a) and 5(b). Besides the final image, inversion results also show clear improvements from the new WATS broadband PSDM data. The uplifting result is due to the combination of wide-azimuth acquisition and specific broadband wide-azimuth processing technology that better utilizes the acquisition effort. The inverted Vp/Vs allows for a new channel interpretation (pointed by the black arrow in Fig. 5(d)) and clearly explains the previous misleading prediction mentioned earlier. The new results better match the well findings.

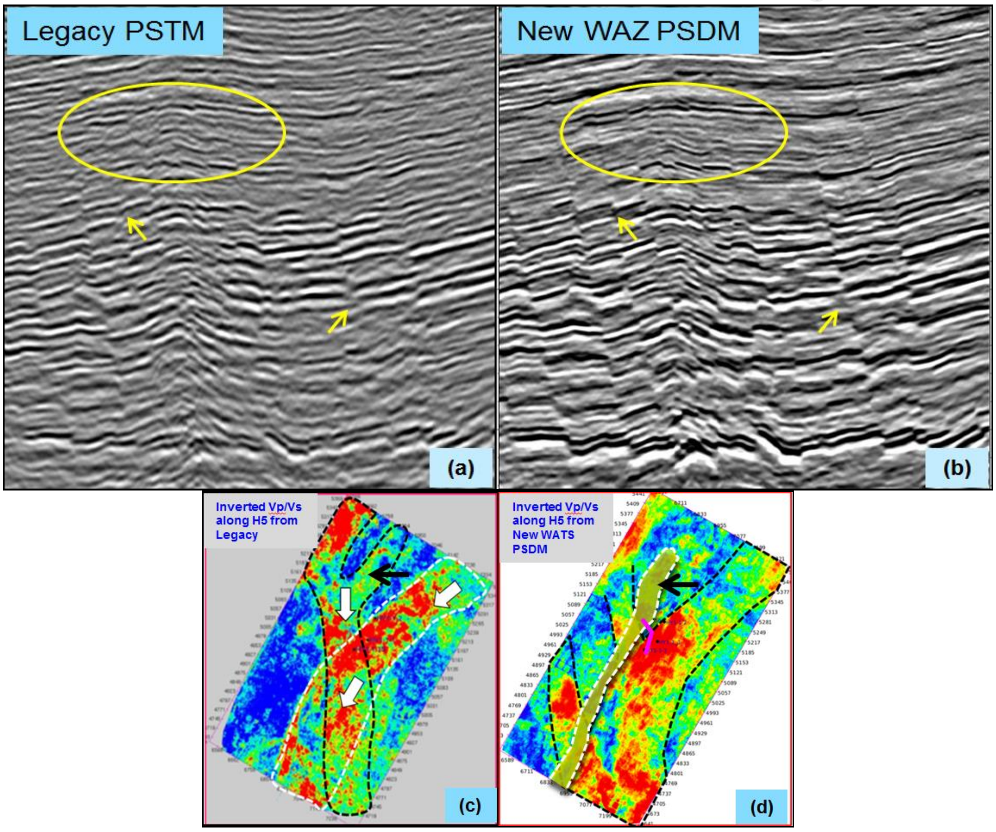

Figure 5: *(a) Legacy PSTM Stack in time; (b) New WAZ PSDM Stack in time; (c) Inverted Vp/Vs from Legacy data at target reservoir with interpretation of two big channels defined by black and white dash lines; (d) Inverted Vp/Vs from New WAZ PSDM Data at target reservoir with interpretation of one big channel defined by black dash lines and one shallower and thinner channel defined by white dash lines with the production well on top (black arrow location).*

Conclusion

A combined solution of advanced 3D processing along with the broadband WATS acquisition successfully resolves the imaging challenges in a shallow water environment with deep targets. Detailed contribution analysis indicates that the 2nd pass side boat can be put closer to the streamer vessel to improve the azimuth distribution as a valuable reference for future survey design.

Acknowledgement

The authors would like to thank CGG and CNOOC for the permission to present this work. Special thanks also go to Yunxin Mao from CNOOC for his inversion work and Todd Woodford, Zhonghuan Chen, and Feng Yang from CGG for reviewing the paper.

Reference:

Michell S, et al. [2006] Wide azimuth streamer imaging of Mad Dog; Have we solved the subsalt imaging problem? *76th Annual Meeting. SEG, Expanded Abstracts*, 2905-2909.

Wang J and Wang S. [2014] Anisotropy-preserving 5D interpolation by hybrid Fourier transform, *2014 GeoConvention: FOCUS, CSEG.*

Wang P, Ray S, Nimsaila K. [2014] 3D joint deghosting and crossline interpolation for marine single-component streamer data, *84th Annual Meeting, SEG, Expanded Abstracts*, 3594-3598.

Wu Q, Lee C C, Zhao W, et al. [2014] 3D deghosting for full-azimuth and ultra-long offset marine data, *84th Annual Meeting. SEG, Expanded Abstracts*, 4238-4242.

VerWest B J, Lin D. [2007] Modeling the impact of wide-azimuth acquisition on subsalt imaging, *Geophysics*, **72**(5), SM241-SM250.